Calhoun
Institutional Archive of the Naval Postgraduate School

Calhoun: The NPS Institutional Archive

DSpace Repository

Faculty and Researchers | Faculty and Researchers Collection

1989

Cloud and ocean mixed layer feedback

Garwood, R.W., Jr.
Chu, Peter C.

Chu, P.C., and R.W. Garwood, Jr., 1989: Cloud and ocean mixed layer feedback. The Role of Clouds in Atmospheric Chemistry and Global Climate, American Meteorological Society, 39-44
http://hdl.handle.net/10945/36259

Downloaded from NPS Archive: Calhoun

http://www.nps.edu/library

Calhoun is a project of the Dudley Knox Library at NPS, furthering the precepts and goals of open government and government transparency. All information contained herein has been approved for release by the NPS Public Affairs Officer.

Dudley Knox Library / Naval Postgraduate School
411 Dyer Road / 1 University Circle
Monterey, California USA 93943

1.9

CLOUD-OCEAN MIXED LAYER FEEDBACK

P.C. Chu and Roland, W. Garwood, Jr.
Naval Postgraduate School
Monterey, California

1. Introduction

A cloud-ocean planetary boundary layer (OPBL) feedback mechanism is presented and tested in this paper: water vapor, evaporated from the ocean surface or transported by the large-scale air flow, often forms convective clouds under a conditionally unstable lapse rate. The variable cloud cover and rainfall may have positive and negative feedback with the ocean mixed layer temperature and salinity structure. First, clouds reduce the incoming solar radiation at the ocean surface by scattering and absorption, which cools (relatively) the ocean surface layer by increasing mixed layer entrainment. The cooling of the ocean mixed layer lowers the evaporation rate, which will diminish the clouds. This is a negative feedback mechanism. Second, precipitation dilutes the surface salinity, stabilizing the upper ocean and reducing mixed layer deepening. The mixed layer may even be caused to shallow if the downward surface buoyancy flux is sufficiently enhanced by the precipitation. The reduction in mixed layer depth will increase the sea surface temperature (SST) by concentrating the net radiation plus heat fluxed downward across the sea surface into a thinner layer. The increase of SST augments the surface evaporation, which in turn produces more clouds. This is a positive feedback mechanism. Fig.1 shows the main physical processes (heat, mass, and momentum fluxes) at the two adjacent boundary layers: the OPBL and the marine atmospheric boundary layer (MABL). Fig.2 illustrates this positive/negative feedback mechanism.

Since clouds have significant effects on the large-scale atmospheric circulation through the transfer of heat, moisture, and momentum, and on the ocean mixed layer through the attenuation of solar radiation at the ocean surface, and since the SST is an important factor for the development of clouds, the feedback mechanism mentioned above has a potentially significant impact on the air-sea interaction, weather and ocean prediction.

The coupled model is one-dimensional. We are aware of the importance of the horizontal advection and the limitation of one-dimensional models. However, the intent of this work is to develop a formalism to examine this thermodynamic feedback between the two fluids. Because we wish to concentrate on the thermodynamic interaction, horizontal advection is ignored initially.

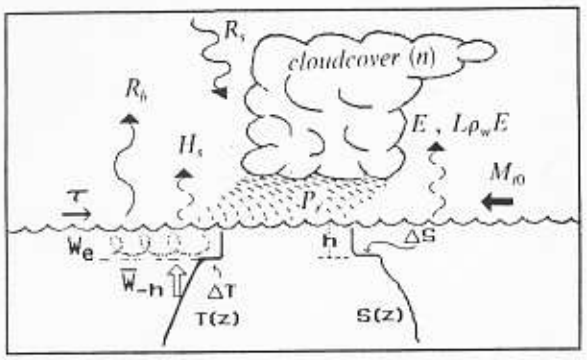

Fig.1 Main physical processes at the two adjacent boundary layers.

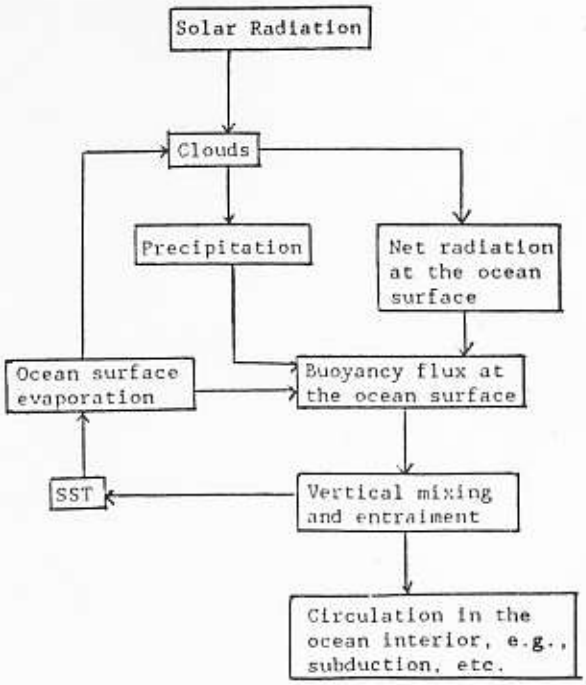

Fig.2 Feedback mechanism between OPBL and clouds.

2. The Oceanic Mixed Layer

2.1 Basic equations

Much of the one-dimensional theory for the OPBL or mixed layer is dependent upon the validity of two crucial hypotheses. The first of these is that vertical mixing within the turbulent boundary layer and entraiment mixing at its base occur in response to the local atmospheric forcing - the surface wind stress and the buoyancy flux at the sea surface. The second hypothesis is that the mechanical energy budget is the key to the understanding and prediction of mixed layer dynamics (Garwood, 1979).

The buoyancy flux is attributable to heat flux, evaporation, and precipitation, and the shear production of turbulence is attributable to surface wind stress. The mixed layer temperature T_s, salinity S_s, and depth h are predicted by a simplified form of the Garwood (1977) mixed layer model. It is essentially a "calibrated" Kraus and Turner (1967) model which is modified to include salinity and advection:

$$h\frac{\partial T_s}{\partial t} = -w_e(T_s - T_{-h}) - \frac{F_T|_{z=0}}{\rho_w c_p^{(w)}} \qquad (1)$$

$$h\frac{\partial S_s}{\partial t} = -w_e(S_s - S_{-h}) + (E - P_r)S_s \qquad (2)$$

where h is the mixed layer depth, $c_p^{(w)}$ is the water specific heat under constant pressure, ρ_w is the characteristic water density, E is the surface evaporation (m/s), P_r is the precipitation rate (m/s), and w_e is the entrainment velocity parameterized as (Chu and Garwood, 1988):

$$w_e = \frac{(C_1 u_*^3 - C_2 B_0 h)}{gh[\alpha(T_s - T_{-h}) - \beta(S_s - S_{-h})]} \tag{3}$$

where u_* is the water surface friction velocity, which is computed by

$$u_* = \left(C_D \frac{\rho_a}{\rho_w}\right)^{0.5} |\vec{V}_0^{(a)}| \tag{4}$$

where C_D is the drag coefficient, taken as 0.001, $|\vec{V}_0^{(a)}|$ is the wind speed at a 10 m height, ρ_a is air density near ocean surface, and ρ_w is the sea water density. For a wind speed of 10 m/s, $u_* \sim 1.1$ cm/s. For the case of an ocean surface without ice (low and middle latitudes) the surface buoyancy flux, B_0, has two components:

$$B_0 = -\frac{\alpha g F_T|_{z=0}}{\rho_w c_p^{(w)}} - \beta g(E - P_r)S_s \tag{5}$$

Here α is the water thermal expansion coefficient, and β is the salinity contraction coefficient.

The effects of clouds on the buoyancy flux at the ocean surface are two-fold: (1) decreasing B_0 through the increase in the net heat loss at the ocean surface, $F_T|_{z=0}$, by reducing the incoming solar radiation, and (2) increasing B_0 due to precipitation.

The surface heat flux $F_T|_{z=0}$ (upward positive), is computed by

$$F_T|_{z=0} = R_b - R_s + L\rho_w E + H_s \tag{6}$$

Here R_s is the incoming solar radiation absorbed by the ocean surface, R_b is the net energy loss from the ocean surface through longwave radiation, L is the latent heat of vaporization of water, H_s is the sensible heat flux to the air. The variables T_{-h} and S_{-h} are the temperature and salinity of the water immediately below the mixed layer that is to be entrained into the mixed layer. The standard bulk formulae are used to calculate the surface evaporation:

$$E = \rho_a C_D |\vec{V}_0^{(a)}|[q_s(T_s) - q_0]/\rho_w \tag{7a}$$

and the sensible heat flux from the ocean surface:

$$H_s = \rho_a c_p^{(a)} C_D |\vec{V}_0^{(a)}|(T_s - T_{a0}) \tag{7b}$$

where q_s(T) is the saturated mixing ratio, and T_{a0} is the air temperature near the ocean surface.

The time rate of change in mixed layer depth is computed by

$$\frac{\partial h}{\partial t} = w_e - w_{-h} \tag{8}$$

where w_{-h} is the upwelling velocity at the bottom of the mixed layer. In order to solve these equations, we should compute each term in the surface heat and salinity fluxes.

2.2 Cloud effects on the net radiation at the ocean surface

Clouds reduce the solar radiation upon the ocean surface by scattering and absorption, which is computed by Budyko's (1978) formula

$$R_s = [1 - \alpha_{sn} n - \alpha_{s0}(1 - n)]R_{s0} \tag{9}$$

Here R_{s0} (340 W m^{-2}) is the solar radiation absorbed by the ocean surface layer under a clear sky. The parameters α_{sn} and α_{s0} represent albedos of the earth-atmosphere system with complete cloud cover and a cloudless sky respectively, and have the following values:

$$\alpha_{sn} = 0.46, \qquad \alpha_{s0} = 0.2$$

The ocean surface emits longwave radiation to the atmosphere and to space. However, clouds, as well as dry air, partially absorb the radiation and re-emit longwave radiation back to the ocean surface. Thus the net upward energy loss by longwave radiation at the ocean surface, R_b, is corrected for the downward radiation by the clouds and the air. From longwave radiation data, Budyko (1978) derived a semi-emprical formula:

$$R_b = a + bT - (a_1 + b_1)n \tag{10}$$

The dimensional coefficients a, b, a_1 , and b_1 are

$$a = -377.6\ Wm^{-2},\ b = 2.2\ Wm^{-2}K^{-1},$$

$$a_1 = -389.8\ Wm^{-2}, b_1 = 1.6\ Wm^{-2}K^{-1}$$

3. Time Rate of Change of the Cloud Cover

The time rate of of change of cloud cover is assumed to be proportional to the moisture supply divided by the amount of water vapor necessary to produce the model cloud. The main processes causing the cloud dissolution are precipitation and mixing with the environmental air. The cloud evaporation due to mixing with ambient air is a complicated problem, and neglected for the sake of simplicity in this paper. Thus the equation for cloud cover is

$$\frac{\partial n}{\partial t} = \frac{(M_{s0} + E - P_r)}{W} \tag{11}$$

where W is the total amount of water vapor needed to create the cloud over a unit area. The large-scale horizontal moisture convergence in the column of atmosphere per unit area is denoted M_{s0}. From mean distributions of temperature and mixing ratio in the environmental air and inside a deep cumulus cloud (Kuo, 1965), we estimate that $W \sim 5$ cm. Eqs. (1), (2), (3), (8), and (11) are the basic equations for the air-ocean coupled system.

4. Relationship between Precipitation Rate and Cloud Cover

By linear regression with use of hourly rain amounts and satellite IR brightness measured during Phase I, II, and III of GATE, Albright et al. (1985) presented a linear relationship between average precipitation rate P_r in boxes 1.5° (168 km) on a side and cloud cover n of the boxes by clouds with tops colder than −36° C. The relationship is

$$P_r(ms^{-1}) = (0.472 + 8.333\ n) \times 10^{-7} \tag{12}$$

This result coincides with Arkin (1979)'s earlier analysis during GATE over the B-scale array.

5. Mean State and Perturbations

Mean state of the coupled cloud-OPBL system $(\overline{T}_s, \overline{S}_s, \overline{h}, \overline{E}, \overline{P}_r, \overline{w}_e)$ is obtained by the zero time rate of change in the prognostic equations (1), (2), (8), and (11). The mean entrainment velocity $\overline{w}_e$ can be obtained from (3)

$$\overline{w}_e = \frac{C_1 \overline{u}_*^3 - C_2 \overline{B}_0 \overline{h}}{\overline{h}\Delta b} \tag{13}$$

where

$$\Delta b \equiv g(\alpha \Delta T - \beta \Delta S)$$

is the reduced gravity, and ΔT and ΔS are the mean temperature and salinity jumps at the bottom of the mixed layer

$$\Delta T \equiv \overline{T}_s - T_{-\overline{h}}, \quad \Delta S \equiv \overline{S}_s - S_{-\overline{h}}$$

When the coupled system is perturbed from its mean state, the thermodynamic feedback mechanism between the cumulus clouds and the oceanic mixed layer makes the perturbation either grow (positive feedback) or dampen (negative feedback). The principal purpose here is to study thermodynamic feedback mechanisms between clouds and the oceanic mixed layer. Hence the energy exchange at the air-ocean interface is a primary focal point. Therefore, we shall neglect initially the perturbations of those variables which are not directly related to the exchange at the air-ocean interface. Wyrtki (1981) estimated that the mean upwelling in the equatorial Pacific is around 1 *m/day*. Climatic data also indicates that the mean evaporation and precipitation rates are on the order of 1 *m/yr* ($3.17 \times 10^{-8} ms^{-1}$). The direct contributions of evaporation and precipitation to the change of mixed layer depth are neglected, compared to the contributions due to upwelling and entrainment.

The perturbations satisfy the following equations:

$$\bar{h}\frac{\partial T'_s}{\partial t} = -\bar{w}_{-h}T'_s - w'_e\Delta T - \frac{F'_T|_{z=0}}{\rho_w c_p^{(w)}} \tag{14}$$

$$\bar{h}\frac{\partial S'_s}{\partial t} = -\bar{w}_{-h}S'_s - w'_e\Delta S + (\bar{E}-\bar{P}_r)S'_s + \bar{S}_s(E'-P'_r) \tag{15}$$

$$\frac{\partial n'}{\partial t} = \frac{1}{W}(E'-P'_r) \tag{16}$$

$$\frac{\partial h'}{\partial t} = w'_e \tag{17}$$

$$w'_e\Delta b = -g\bar{w}_{-h}(\alpha T'_s - \beta S'_s) - C_1\frac{\bar{u}^3}{\bar{h}^2}h'$$
$$+ C_2\left[\frac{\alpha g F'_T|_{z=0}}{\rho_w c_p^{(w)}} + \beta g\bar{S}_s(E'-P'_r) + \beta g(\bar{E}-\bar{P}_r)S'_s\right] \tag{18}$$

Eliminating h', w'_e, E', P'_r from (14)-(18) and neglecting the small terms, we get the following fourth order equation for each variable:

$$\left(\frac{\partial^4}{\partial t^4} + a_1\frac{\partial^3}{\partial t^3} + a_2\frac{\partial^2}{\partial t^2} + a_3\frac{\partial}{\partial t} + a_4\right)(\phi', n') = 0 \tag{19}$$

where

$$\phi' \equiv \beta S'_s - \alpha T'_s$$

$$a_1 \equiv \frac{1}{\tau_w} + \frac{C_1}{Ri\tau_t} + \frac{\gamma}{W}$$

$$a_2 \equiv -\frac{m\kappa}{\tau_e}\left(C_2 + \frac{1}{\kappa}\right)\lambda + \frac{2C_1}{Ri\tau_t\tau_w} + \left(\frac{m\beta\bar{S}_s}{\tau_e} + \frac{C_1}{Ri\tau_t}\right)\frac{\gamma}{W}$$

$$a_3 \equiv -\frac{m}{\tau_w\tau_e}(1+C_2)\kappa\lambda - \frac{C_1 m\lambda}{Ri\tau_e\tau_t} + \frac{C_1}{Ri\tau_t}\left(\frac{m\beta\bar{S}_s}{\tau_e} + \frac{2}{\tau w}\right)\frac{\gamma}{W}$$

$$a_4 \equiv \frac{C_1}{Ri\tau_t\tau_w^2}\left[-\frac{m\tau_w}{\tau_e}\lambda + (1+m\beta\bar{S}_s\frac{\tau_w}{\tau_e})\frac{\gamma}{W}\right] \tag{20}$$

Here three constants τ_w, τ_t, τ_e are time-scales of internal motion, ocean turbulence, and surface evaporation defined by

$$\tau_w \equiv \frac{\bar{h}}{\bar{w}_{-h}}, \quad \tau_t \equiv \frac{\bar{h}}{\bar{u}_*}, \quad \tau_e \equiv \frac{\bar{h}}{\mu} \tag{21}$$

where

$$\mu \equiv \frac{L}{c_p^{(w)}}\frac{\partial E}{\partial T}|_{\bar{T}_s} = \frac{L\rho_a C_D|\vec{V}_0^{(a)}|}{\rho_w c_p^{(w)}}\frac{dq_s(\bar{T}_s)}{dt} = 0.5\times 10^{-5} ms^{-1} \tag{22}$$

The constants γ and m are defined by

$$\gamma \equiv \frac{\partial P_r}{\partial n}|_{\bar{n}}, \quad m \equiv \frac{c_p^{(w)}}{\alpha L} = 8.5 \tag{23a}$$

Using (11) we have

$$\gamma = 8.333\times 10^{-7} ms^{-1} \tag{23b}$$

Ri is the Richardson number

$$Ri \equiv \frac{\Delta b\tau_t^2}{\bar{h}} \tag{23c}$$

In this paper *Ri* is taken as 10^4. The two model parameters λ, and κ are defined by

$$\lambda \equiv \frac{1}{gW}\frac{\partial B_0}{\partial n} \tag{24a}$$

which is the dependence of the surface buoyancy flux change on cloud cover, and

$$\kappa \equiv \frac{\alpha g\Delta T}{\Delta b} \tag{24b}$$

which is the fraction of the mixed layer base density jump induced by temperature to the total density jump.

6. Instability and Oscillation Criteria

The general solutions of (19) have the following forms:

$$\phi'(t) = \Sigma d_j\exp(\sigma_j t), \quad n'(t) = \Sigma e_j\exp(\sigma_j t) \tag{25}$$

where d_j, e_j (j = 1,2,3,4) are the integral constants, and σ_1, σ_2, σ_3, and σ_4 are the eigenvalues which are the roots of the fourth-order algebraic equation,

$$\sigma^4 + a_1\sigma^3 + a_2\sigma^2 + a_3\sigma + a_4 = 0 \tag{26}$$

For the purpose of a preliminary sensitivity analysis only κ and λ are allowed to vary, depending on observations. Other parameters are given constant values listed in Table 1. By the definition of λ (24a) and the estimations of γ (23b) and Budyko's formulae (8,9) we can estimate the value of λ as

$$\lambda \sim 0.45\times 10^{-6} s^{-1} \tag{27}$$

which indicates that λ has an order of $10^{-6}s^{-1}$. Therefore in this paper, λ varies from $-10^{-6}s^{-1}$ to $10^{-6}s^{-1}$. It is reasonable to let κ vary between -10 to 10. The case of $\kappa = 1$ means that salinity is homogeneous across the mixed layer base.

The instability criteria for the thermodynamically coupled air-ocean system are

$$Re(\bar{\sigma}) \begin{cases} < 0 & decaying \\ = 0 & neutral, \\ > 0 & growing \end{cases} \tag{28}$$

where $\bar{\sigma}$ is the root of the fourth-order equation (26). The oscillatia criterion for the coupled system are

$$Im(\bar{\sigma}) \begin{cases} = 0 & nonoscillatory \\ \neq 0 & oscillatory \end{cases} \tag{29}$$

We compute all roots of (26) for different values of the parameters κ and λ, and obtain four roots at each points of the parameter space (κ, λ). Two roots among the four have negative real parts throughout the whole parameter space, representing the damping modes, in which we are not interested here. The other two roots, σ_1 and σ_2, have positive real parts somewhere in the parameter space, representing the existence of growing modes in certain parameter ranges.

Table 1 The values of the model parameters

ρ_a	$1.29\ kg/m^3$	C_1	1.0	$\lvert\vec{V}_0^{(a)}\rvert$	$10\ m/s$
ρ_w	$1035\ kg/m^3$	C_2	0.2	$\overline{T}_s$	$20^\circ C$
α	$0.2\times10^{-3}K^{-1}$	C_D	10^{-3}	$\overline{S}_s$	$35\ g/kg$
β	0.8×10^{-3}	W	$5cm$	$\overline{h}$	$50\ m$
		$\overline{n}$	0.5	$\overline{w}_{-h}$	$1\ m/day$

Fig.3 shows the isolines of (a) $Re(\sigma_1)$ and (b) $|Im(\sigma_1)|$ in the (κ, λ) plane. Fig.4 indicates the isolines of (a) $Re(\sigma_2)$ and (b) $|Im(\sigma_2)|$ in the (κ, λ) plane. Both the real part (growth rate) and the absolute value of the imaginary part (periodicity) of the roots σ_1, σ_2 show saddle-type distributions. Several interesting results from Figs.3 and 4 are summarized as follows:

1. A necessary condition for the generation of growing modes, which can be seen from these figures, is:

$$\kappa\lambda > 0 \tag{30}$$

This implies that if the surface water is warmer (cooler) than the deep water, i.e., $\kappa > 0$ ($\kappa < 0$), the growing modes are excited. In this case that the surface buoyancy flux increases with increasing (decreasing) cloud cover.

2. If the damping modes are ignored, the two eigenvalues σ_1 and σ_2 exhibit the similar properties. The growing modes, σ_1 and σ_2, are further separated into oscillatory and nonoscillatory modes. The condition for this separation is approximately given by

$$\kappa\lambda \begin{cases} < \Lambda & Oscillatory \\ > \Lambda & Nonoscillatory \end{cases} \tag{31}$$

where Λ is a positive number of about $2\times10^{-6}s^{-1}$.

Combining (30) with (31) and using (24a), the necessary condition for oscillatorily growing modes is

$$\Lambda > \frac{\kappa}{W}\frac{\partial}{\partial n}\left[\beta\overline{S}_s P_r - \frac{\alpha(R_b - R_s)}{\rho_w c_p^{(w)}}\right]\Big|_{\overline{T}_s,\overline{n}} > 0 \tag{32}$$

and the condition for the nonoscillatorily growing modes is

$$\frac{\kappa}{W}\frac{\partial}{\partial n}\left[\beta\overline{S}_s P_r - \frac{\alpha(R_b - R_s)}{\rho_w c_p^{(w)}}\right]\Big|_{\overline{T}_s,\overline{n}} > \Lambda \tag{33}$$

The properties of thermodynamic instability of the coupled system depend largely on the relationship between precipitation P_r and the cloud cover, and on the relationship between net radiation at the ocean surface and the cloud cover.

3. The product of the two parameters κ and λ represents the relative strength of positive to negative feedback. When $\kappa\lambda$ is larger than the critical value Λ, the positive feedback greatly exceeds the negative feedback. The coupled system becomes nonoscillatory and growing. When $\kappa\lambda$ is positive and smaller than the critical value Λ, the positive feedback slightly exceeds the negative feedback. The coupled system is oscillatory and growing. When $\kappa\lambda$ is negative, the negative feedback exceeds the positive feedback. The coupled system becomes damping. Comparing Fig.4 with Fig.3, we find that for the oscillatorily growing modes the two roots have the same growth rate and frequency. However, for the nonoscillatorily growing modes the growth rate relating to the eigenvalue σ_2 is much larger than that relating to σ_1.

4. For the oscillatorily growing modes, the growth rate σ_r has the order of $0.5\times10^{-7}s^{-1}$, and $|\sigma_i|$ has the order of $10^{-7}s^{-1}$. The corresponding period for the oscillation is

$$T = \frac{2\pi}{|\sigma_i|} = 2\ yr \tag{34}$$

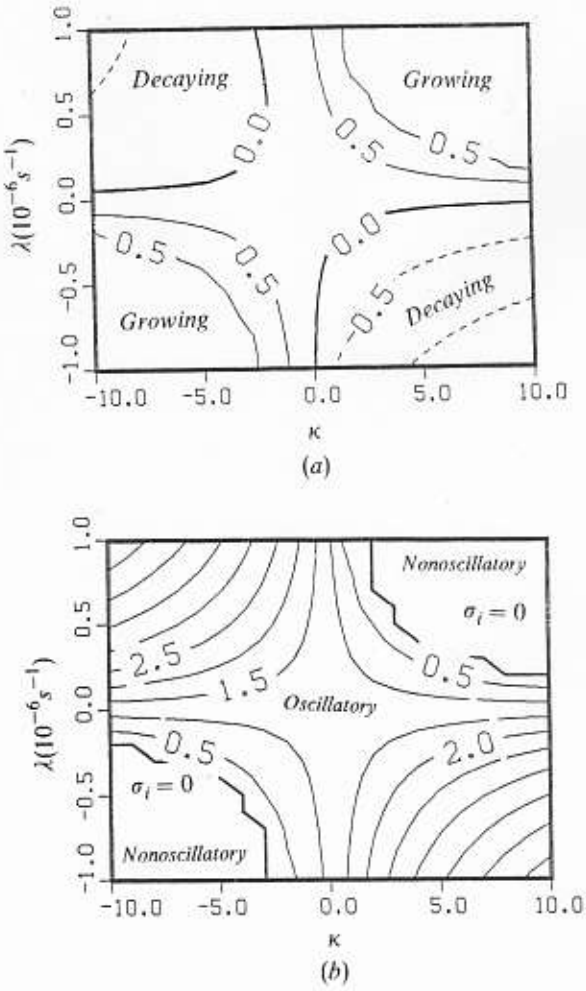

Fig.3 Distribution of eigenvalue σ_1 in the (κ, λ) plane for standard case (unit in $10^{-7}s^{-1}$): (a) $\mathrm{Re}(\sigma_1)$, (b) $|\mathrm{Im}(\sigma_1)|$.

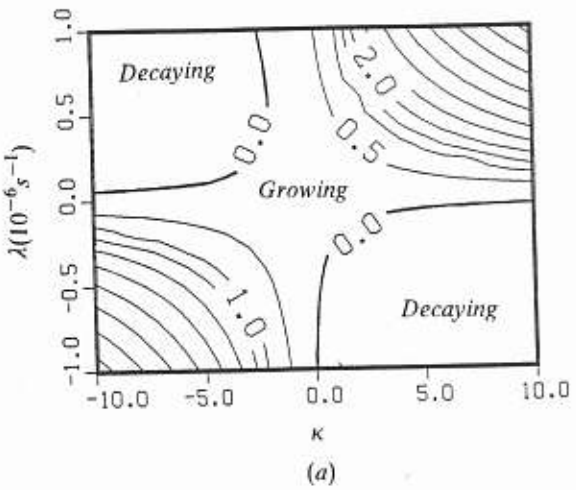

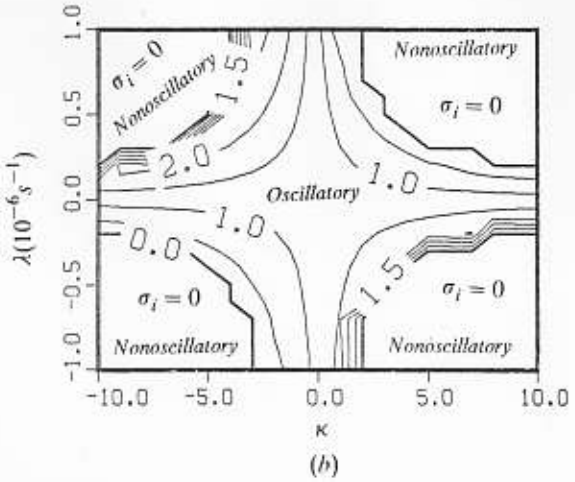

Fig.4 Distribution of eigenvalue σ_2 in the (κ, λ) plane for standard case (unit in $10^{-7}s^{-1}$): (a) $\mathrm{Re}(\sigma_2)$, (b) $|\mathrm{Im}(\sigma_2)|$.

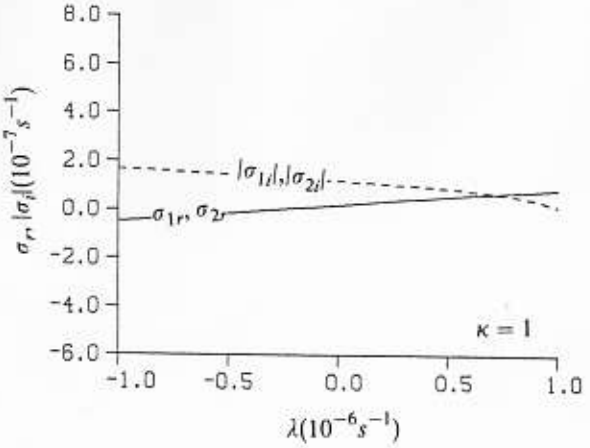

Fig.5 Dependence of $(\sigma_{1r}, |\sigma_{1i}|)$ and $(\sigma_{2r}, |\sigma_{2i}|)$ on λ for the case without salinity jump at the mixed layer base.

7. Sensitivity of σ_r, $|\sigma_i|$ to λ and κ

In order to investigate the dependence of σ_r and $|\sigma_i|$ on the parameters κ and λ, we plot σ_{1r}, σ_{2r}, $|\sigma_{1i}|$, $|\sigma_{2i}|$ versus λ at five different values of κ ($\kappa = 1, 5, 10, -5, -10$), and taking the same values for the parameters as in Table 1. The results are listed below.

1. Fig.5 represents the case for $\kappa = 1$, i.e., the case with no salinity jump at the mixed layer base. The identity of $(\sigma_{1r}, |\sigma_{1i}|)$ to $(\sigma_{2r}, |\sigma_{2i}|)$ means the two eigenvalues are complex conjugates. Fig.5 shows that the growth rate σ_r is a linearly increasing function of λ from $\sigma_r = -0.5 \times 10^{-7}s^{-1}$ (damping mode) for $\lambda = -10^{-6}s^{-1}$ to $\sigma_r = 0.5 \times 10^{-7}s^{-1}$ (growing mode) for $\lambda = 0.5 \times 10^{-6}s^{-1}$. The frequency $|\sigma_i|$ decreases almost linearly with λ from $|\sigma_i| = 1.7 \times 10^{-7}s^{-1}$ (1.2 year period) for $\lambda = -10^{-6}s^{-1}$ to $|\sigma_i| = 0.86 \times 10^{-7}s^{-1}$ (2.3 year period) for $\lambda = 0.5 \times 10^{-6}s^{-1}$.
2. The dependence of growth rates σ_{1r}, σ_{2r} and frequencies $|\sigma_{1i}|$, $|\sigma_{2i}|$ on λ for $\kappa = 5$ and $\kappa = 10$ is depicted in Fig.6. The value of σ_{2r} monotonically increases with λ, whereas σ_{1r} has a single peak which is around $0.5 \times 10^{-7}s^{-1}$, and asymptotically tends to zero as $\lambda \to +\infty$. The necessary condition for the growing oscillation is

$$0 < \lambda < \lambda_c \tag{35}$$

where $\lambda_c = \frac{A}{\kappa}$, is a critical value for λ.

8. Sensitivity of σ_r, $|\sigma_i|$ to $\bar{w}_{-h}$

To understand the dependence of σ_r and $|\sigma_i|$ on the mean vertical velocity at the mixed layer base, $\bar{w}_{-h}$, we compute the roots of (26) by using the same values for the parameters as previous two sections except for $\bar{w}_{-h}$, which is changed to two alternate values: $\bar{w}_{-h} = 0.2m/day$ (weak upwelling case) and $\bar{w}_{-h} = 2m/day$ (strong upwelling case).

The main results are that the growth rate and the frequency of the coupled system are strongly affected by the vertical advection, and the larger the $\bar{w}_{-h}$, the bigger the value of σ_r, and the higher the frequency, $|\sigma_i|$.

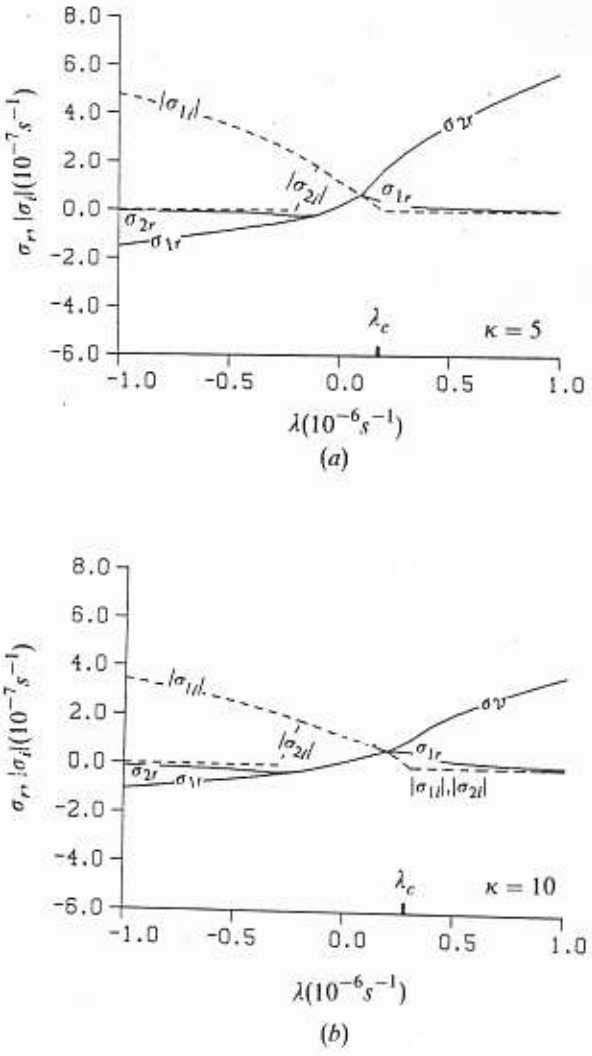

Fig.6 Dependence of $(\sigma_{1r}, |\sigma_{1i}|)$ and $(\sigma_{2r}, |\sigma_{2i}|)$ on λ for (a) $\kappa = 5$, (b) $\kappa = 10$.

9. Conclusions

A coupled cloud-OPBL thermodynamic model has been presented. This model demonstrates the positive/negative feedback mechanisms between clouds and ocean mixed layer, including salinity effects. The theory predicts the generation of biennial growing oscillations at typical ranges of initial states in the tropical ocean and atmosphere, which may provide a new explanation for the low frequency oscillation in the atmosphere and oceans.

Acknowledgements.

This research was supported jointly by the National Science Foundation (NSF) under NSF Grant OCE85-15400, and by the Naval Postgraduate School (NPS) through Research Foundation Fund.

REFERENCES

Albright, M.D., E.E. Recker, R.J. Reed, and R.Q. Dang, 1985: The diurnal variation of deep convection and inferred precipitation in the central tropical Pacific during January-February 1979. Mon. Wea. Rev., 113, 1663-1680.

Arkin, P.A., 1979: The relationship between fractional coverage of high cloud and rainfall accumulations during GATE over the B-scale array. Mon. Wea. Rev., 107, 1382-1387.

Budyko, M.I., 1978: The heat balance of the earth. Climatic Change (ed. J. Gribbin), Cambgidge Univ. Press, 85-113.

Chu, P.C., and R.W. Garwood, Jr., 1988: Comment on "A coupled dynamic-thermodynamic model of an ice-ocean in the marginal ice zone" by Sirpa Hakkinen. J. Geophys. Res., 93, 5155-5156.

Garwood, R.W. Jr., 1977: An oceanic mixed layer capable of simulating cyclic states. J. Phys. Oceanogr., 7, 455-468.

Garwood, R.W. Jr., 1979: Air-sea interaction and dynamics of the surface mixed layer. Rev. Geophys. Space Phys., 17, 1507-1524.

Kraus, E.B., and J.S. Turner, 1967: A one-dimensional model of the seasonal thermocline, Part II. Tellus, 19, 98-105.

Kuo, H.L., 1965: On formation and intensification of tropical cyclones through latent heat release by cumulus convection. J. Atmos. Sci., 22, 40-63.

Wyrtki, K., 1981: An estimation of equatorial upwelling in the Pacific. J. Phys. Oceanogr., 11, 1205-1214.